Nonlinear development of the R-mode instability and the maximum rotation rate of neutron stars

Bondarescu, Ruxandra ; Wasserman, Ira

Abstract: We describe how the nonlinear development of the R-mode instability of neutron stars influences spin up to millisecond periods via accretion. When nearly resonant interactions of the l = m = 2 R-mode with pairs of "daughter modes" are included, the R-mode saturates at the lowest amplitude which leads to significant excitation of a pair of modes. The lower bound for this threshold amplitude is proportional to the damping rate of the particular daughter modes that are excited parametrically. We show that if dissipation occurs in a very thin boundary layer at the crust-core boundary, the R-mode saturation amplitude is too large for angular momentum gain from accretion to overcome loss to gravitational radiation. We find that lower dissipation is required to explain spin up to frequencies much higher than 300 Hz. We conjecture that if the transition from the fluid core to the crystalline crust occurs over a distance much longer than 1 cm, then a sharp viscous boundary layer fails to form. In this case, damping is due to shear viscosity dissipation integrated over the entire star. We estimate the lowest parametric instability threshold from first principles. The resulting saturation amplitude is low enough to permit spin up to higher frequencies. The requirement to allow continued spin up imposes an upper bound to the frequencies attained via accretion that plausibly may be about 750 Hz. Within this framework, the R-mode is unstable for all millisecond pulsars, whether accreting or not.

DOI: https://doi.org/10.1088/0004-637X/778/1/9

Draft version September 6, 2013
Preprint typeset using LaTeX style emulateapj v. 5/2/11

NONLINEAR DEVELOPMENT OF THE R MODE INSTABILITY AND THE MAXIMUM ROTATION RATE OF NEUTRON STARS

Ruxandra Bondarescu
Institute for Theoretical Physics, University of Zurich, CH-8057, Switzerland

and

Ira Wasserman[1]
Center for Radiophysics and Space Research, Cornell University, Ithaca, NY 14853

Draft version September 6, 2013

ABSTRACT

We describe how the nonlinear development of the R mode instability of neutron stars influences spin up to millisecond periods via accretion. Our arguments are based on nearly-resonant interactions of the R mode with pairs of "daughter modes." The amplitude of the R mode saturates at the lowest value for which parametric instability leads to significant excitation of a particular pair of daughters. The lower bound on this limiting amplitude is proportional to the damping rate of the daughter modes that are excited parametrically. Based on this picture, we show that if modes damp because of dissipation in a very thin boundary layer at the crust-core boundary then spin up to frequencies larger than about 300 Hz does not occur. Within this conventional scenario the R mode saturates at an amplitude that is too large for angular momentum gain from accretion to overcome gravitational loss to gravitational radiation. We conclude that *lower* dissipation is required for spin up to frequencies much higher than 300 Hz. We conjecture that if the transition from the fluid core to the crystalline crust occurs over a distance much longer than ~ 1 cm then a sharp viscous boundary layer fails to form. In this case, damping is due to shear viscosity dissipation integrated over the entire star; the rate is slower than if a viscous boundary layer forms. We use statistical arguments and scaling relations to estimate the lowest parametric instability threshold from first principles. The resulting saturation amplitudes are low enough to permit spin up to higher frequencies. Further, we show that the requirement that the lowest parametric instability amplitude be small enough to allow continued spin up imposes an upper bound to the frequencies that may be attained via accretion that may plausibly be about 750 Hz. Within this framework, the R mode is unstable for *all* millisecond pulsars, whether accreting or not.

1. THE R MODE INSTABILITY VERSUS THE SPIN UP LINE

The fastest spinning radio pulsar has a rotational frequency $\nu = 716$ Hz (Hessels et al. 2006) and 39 have been detected with $\nu > 400$ Hz (Manchester et al. 2005). See ATNF Pulsar Catalogue at `http://www.atnf.csiro.au/research/pulsar/psrcat/`. Moreover, there are 14 pulsars in X ray binaries with inferred $\nu > 400$ Hz, but none demonstrated convincingly to be faster than 620 Hz (Watts 2012; Patruno & Watts 2012); Chakrabarty has argued that the population of neutron star spins cuts off sharply at around 730 Hz (Chakrabarty 2005, 2008, 2012). In the standard picture, millisecond pulsars are thought to be spun up via accretion (Alpar et al. 1982) and the $P - \dot{P}$ diagram for radiopulsars is consistent with the idea that accreting neutron stars reach spin equilibrium (e.g. Bildsten et al. 1997) in that there appear to be no neutron stars outside the boundary set by the "spinup line" (e.g. Arzoumanian et al. 1999)

$$\nu_{eq} = \frac{\omega_s}{2\pi}\sqrt{\frac{GM}{R_{acc}^3}} \approx \frac{760\,\mathrm{Hz}\,\omega_s \dot{M}_9^{3/7} M_{1.4}^{5/7}}{{\eta_{\rm acc}}^{3/2}\mu_{26}^{6/7}} \qquad (1)$$

where the accretion radius is $R_{acc} \approx 20\eta_{\rm acc}\mu_{26}^{4/7}\dot{M}_9^{-2/7}M_{1.4}^{1/7}$ km, $\dot{M} = 10^{-9}\dot{M}_9 M_\odot\,\mathrm{y}^{-1}$ is the mass accretion rate, $M = 1.4M_{1.4}M_\odot$ is the stellar mass, $\mu = 10^{26}\mu_{26}\,\mathrm{G\,cm}^3$ is the stellar magnetic moment, and $\omega_s \simeq 1$ and $\eta_{\rm acc} \simeq 1$ are parameters that are determined by the magnetohydrodynamics of disk accretion. However, there is no particular reason for there to be a spin frequency cutoff as low as 730 Hz: although there are exceptions, for most representative equations of state of dense nuclear matter accretion can spin up a neutron star from $M = 1.4M_\odot$ and $\nu = 0$ to $\nu \approx 1000 - 1500$ Hz before instability ensues (e.g. Cook et al. 1994).

The R mode instability can prevent neutron stars from spinning up to such high frequencies that either dynamical instability or viscosity-driven secular instability occurs. The R mode instability, which is driven slowly by gravitational radiation but stabilized by viscosity, is reviewed briefly below. However, in the presence of a crust-core boundary layer the R mode prevents spin-up too efficiently: instability sets in at $\nu \approx 300$ Hz (see Eq. (4)), which is too low to allow for observed frequencies of up to 716 Hz since nonlinear effects prevent substantial spin-up while the star is unstable. We call this "*The Spin-Up Problem*": Phenomenologically, the absence of millisecond pulsars outside the spin up line up to at least 660 Hz and the inference that some LMXBs are spinning

ruxandra@physik.uzh.ch
ira@astro.cornell.edu
[1] On leave at KITP UC Santa Barbara

faster than 500 Hz suggest that spin up via slow equilibrium accretion is responsible for the highest spin frequencies observed, but the R mode instability appears to suppress spin up beyond about 300 Hz.

2. R MODE DYNAMICS AND THE SPIN UP PROBLEM

The inertial modes of a rotating star may be thought of as zero frequency "gauge modes" of a *non*rotating star ($\delta\rho = -\boldsymbol{\nabla}\cdot(\rho\boldsymbol{\xi}) = 0$) that acquire frequencies $|\omega| \leq 2\Omega$ in a rotating star to $\mathcal{O}(\Omega)$ (Papaloizou & Pringle 1978; Friedman & Schutz 1978; Lee & Strohmayer 1996; Schenk et al. 2002); the $\ell = |m|$ R modes are a subset that are axial to $\mathcal{O}(1)$ for Newtonian stars, and have (rotating frame) frequencies $|\omega| = 2\Omega/(\ell+1)$. (Relativistic modifications have been discussed by Lockitch et al. (2000).) For the R modes, $\mathcal{O}(1)$ displacement fields can be expressed in terms of a single (magnetic) vector spherical harmonic; decompositions of the other inertial modes are more complicated even at $\mathcal{O}(1)$, generally involving a sum of vector spherical harmonics up to a maximum ℓ (e.g. Lockitch & Friedman 1999; Yoshida & Lee 2000a, 2001; Lockitch et al. 2000, 2003).

The R-modes of rotating neutron stars are destabilized by the emission of gravitational radiation because their rotating and inertial frame frequencies have opposite signs, implying that the rotating frame energy increases as the star radiates energy and angular momentum in the inertial frame (Chandrasekhar 1970; Friedman & Schutz 1978; Andersson 1998; Friedman & Morsink 1998; Lindblom et al. 1998; Bildsten 1998; Andersson et al. 1999). For the most unstable $\ell_R = m_R = 2$ R mode the instability grows at a rate (numerical coefficients are for the Newtonian $N = 1$ polytrope)

$$\gamma_{GR} \approx \frac{M_{1.4}R_{10}^4\nu_{500}^6}{2900\mathrm{s}} \approx 1.6\times10^{-7}M_{1.4}R_{10}^4\nu_{500}^5\,\omega_R \quad (2)$$

where $M = 1.4M_{1.4}M_\odot$ and $R = 10R_{10}$ km are the stellar mass and radius, and $\nu = 500\nu_{500}\,\mathrm{Hz}$; $\omega_R = 2\Omega/3 = 4\pi\nu/3$ (Andersson 1998; Friedman & Morsink 1998; Lindblom et al. 1998; Bildsten 1998; Andersson et al. 1999).

Viscous effects (and other forms of dissipation) act against the instability; the "CFS stability curve" in the frequency-temperature ($\nu - T$) plane separates stable and unstable states (e.g Lindblom et al. 1998; Andersson et al. 1999; Bildsten & Ushomirsky 2000; Lindblom & Owen 2002; Nayyar & Owen 2006; Haskell et al. 2009). For accreting neutron stars spinning up toward the CFS stability curve, balancing accretional heating (e.g. Brown 2000) against neutrino cooling implies internal temperature $T \sim 10^8$K (e.g. Yakovlev & Pethick 2004; Yakovlev et al. 2008; Page et al. 2009). At such low temperatures, dissipation in a viscous boundary layer at the interface between the stellar crust and core is thought to dominate for the R mode (e.g. Bildsten & Ushomirsky 2000) implying that the mode first becomes unstable at a spin frequency

$$\nu_S \approx 340\,\mathrm{Hz}\,(\rho_{b,14}/T_{S,8})^{2/11} \times[10S_R(r_b/0.9R)/M_{1.4}R_{10}]^{4/11}K_4^{1/11}\ , \quad (3)$$

where $\rho_b = 10^{14}\rho_{b,14}\,\mathrm{g\,cm^{-3}}$ is the density at the crust-core boundary, which is at radius r_b, and $\eta_b = 10^4K_4T_8^{-2}\,\mathrm{cm^2\,s^{-1}}$ is the kinematic viscosity at r_b, and $T_S = 10^8T_{S,8}$ K is the temperature. The quantity S_R measures the imperviousness of the crust to penetration by the R mode; it depends primarily on the shear modulus of the crust, but may also be altered by magnetic effects and compressibility (Levin & Ushomirsky 2001; Mendell 2001; Kinney & Mendell 2003; Glampedakis & Andersson 2006). Levin & Ushomirsky (2001) estimate that for the (most unstable) R-mode $S_R \approx 0.1c_{t,8}/R_{10}\nu_{500}$ where $c_t = 10^8c_{t,8}\,\mathrm{cms^{-1}}$ is the speed of crustal shear waves. The various input parameters are somewhat uncertain. For example recent calculations of the shear viscosity in the core of a neutron star with improved treatment of dynamical screening change η_b by a factor of a few and also alter its temperature scaling compared to "traditional" expressions (Cutler et al. 1990; Andersson et al. 2005; Shternin & Yakovlev 2008). While these refinements alter Eq. (4) slightly, the weak viscosity dependence, $K_4^{1/11}$, still implies that ν_S is well below 716 Hz.

The small value of ν_S would not be problematic if spinup were to continue largely unabated within the unstable regime. However, detailed nonlinear three mode evolutions using representative input physics do not support this: the stellar frequency changes little (Bondarescu et al. 2007).

Two basic principles emerged from our work on multimode (Schenk et al. 2002; Brink et al. 2004, 2005) and three mode (Bondarescu et al. 2007, 2009) nonlinear models for saturation of the R mode instability:

1. The R mode amplitude does not grow beyond the first or second lowest parametric instability threshold amplitude $|C_R|_{\rm PIT}$ for interactions with a pair of daughter modes. $|C_R|_{\rm PIT}$ depends on the detuning $\delta\omega = \omega_R - \omega_2 - \omega_3$ between the R mode (ω_R) and daughter ($\omega_{2,3}$) frequencies, the damping rates of the daughters ($\gamma_{2,3}$) and the three mode coupling κ,

$$|C_R|^2_{\rm PIT} = \frac{\gamma_2\gamma_3}{4\kappa^2\omega_2\omega_3}\left[1+\left(\frac{\delta\omega}{\gamma_2+\gamma_3}\right)^2\right] \equiv \frac{9}{4(\kappa_D\Omega)^2}\left[\gamma_D^2+\frac{(\delta\omega)^2}{4}\right]\ . \quad (4)$$

   Parity and triangle selection rules for the interactions require that the principal mode numbers of the daughters satisfy the constraint $n_3 = n_2 \pm 1$, and for large n_i we expect the viscous damping rates of the daughter modes to have similar values $\gamma_i \approx \gamma_D$ ($i = 2, 3$); we have also defined $4\omega_2\omega_3\kappa^2 = \omega_R^2\kappa_D^2 = 4\Omega^2\kappa_D^2/9$.

2. Dissipation of the multitude of daughter modes heats the star a rate

$$H_R = 2MR^2\Omega^2\gamma_{GR}|C_R|^2\ . \quad (5)$$

   Heating proceeds until balanced by cooling, whereupon evolution tends to settle onto curves in the $\nu - T$ plane where thermal balance is maintained.

The first basic principle is a consequence of the relatively sparse couplings of the R mode to the sea of daughters

(Schenk et al. 2002; Brink et al. 2004, 2005) and the second merely says that once a steady cascade is set up the rate at which the R mode sends energy down to the sea equals the rate of linear growth of its (rotating frame) energy. We stress that these two principles are based on the *physics of mode coupling*. Conclusions based on them are more realistic than those based on *ad hoc* prescriptions for nonlinear truncation of the growth of the R mode amplitude.

These two principles lead to generic evolution in the $\nu - T$ plane. The star spins up stably via accretion until it intersects the stability boundary at ν_S and T_S.The R mode amplitude then grows rapidly (Eq. [2]) and reaches $|C_R|_{\rm PIT}$ almost immediately. For reasonable parameters, the R mode heating quickly dominates over accretional heating, and the star heats up to $T > T_S$. Because the cooling, which is dominated by Cooper pair formation at $T_8 \simeq 1$ (e.g. Flowers et al. 1976; Yakovlev et al. 1999; Kolomeitsev & Voskresensky 2008; Page et al. 2009), accelerates rapidly, fast heating of the star halts eventually. Subsequently, the star evolves relatively slowly along a track where heating and cooling are in balance. Whether the star ascends the curve to higher spin frequency or simply descends to lower spin frequency depends on whether the spindown due to gravitational radiation emission is faster or slower than accretional spinup when heating and cooling first balance. If the R mode amplitude at this point is large enough, the star will simply spin down toward the stability curve, intersecting at ν slightly below ν_S; otherwise, the star spins up until gravitational radiation spindown balances accretional spinup. But even in the latter case, Bondarescu et al. (2007) found that when damping in a shearing boundary layer dominates the dissipationevolutionary tracks never wander very far from ν_S. Moreover, once accretion ceases, the star spins down along the curve where heating and cooling balance, so the end point is virtually the same as if there were no spin-up in the unstable regime.

Thus, we have two aspects of the *Spin Up Problem*:

1. The star crosses into the unstable regime at a spin frequency of about 300 Hz.

2. Saturation of the R mode instability prevents spin up to higher frequency.

The physical reasons that the evolution is constrained so tightly can be understood from considering three different characteristic R mode amplitudes:

1. From Eq. (5), the lowest parametric instability threshold is $|C_R|_{\rm PIT} \gtrsim 3\gamma_D/2\Omega$. For damping in a shearing boundary layer this inequality implies

$$|C_R|_{\rm PIT} \gtrsim \frac{3\gamma_D}{2\kappa_D\Omega} \approx \frac{3S_D^2\ell(dE_D/dr)_b}{4\kappa_D E_D} \approx \frac{1.3\times10^{-6}S_D^2K_4^{1/2}(RdE_D/dr)_b}{\kappa_D T_8\nu_{500}^{1/2}R_{10}E_D}. \quad (6)$$

Here $S_D < 1$ is the fractional velocity jump across the crust-core boundary for daughter mode D, and $\ell = (\eta_b/\Omega)^{1/2}$ is the boundary layer thickness. At principal mode numbers $n_D \gtrsim \omega R/c_t \approx 30\nu_{500}R_{10}/c_{t,8}$, where c_t is the transverse shear mode speed in the crust, we expect $S_D \approx 1$; for lower n_D, $S_D < 1$. The fractional velocity jump for the $n = 3$ R-mode is $S_R \approx 0.1$. The lowest $|C_R|_{\rm PIT}$ arises from modes with $\delta\omega \lesssim \gamma_D$, which are likeliest at large n. Explicit evaluation for modes of an incompressible star as well as WKB calculations for a compressible star imply that $(R/E_D)(dE_D/dr)_b$ is independent of n_D for $n_D \gg 1$ (see Appendix A.4). For incompressible stars, calculations by Brink (2005) show that $|\kappa_D| \lesssim 1$ is insensitive to n_D, although larger values are likelier at large n_D; moreover, κ_D is independent of Ω (see Schenk et al. 2002; Arras et al. 2003). Thus, the lower bound in Eq. (7) is roughly independent of n_D. In fact, because the lowest expected $\delta\omega$ decreases with n while γ_D is roughly independent of n_D, ultimately $|C_R|_{\rm PIT} \simeq 3\gamma_D/2\kappa_D\Omega$ is the lowest parametric instability threshold for damping in a shearing boundary layer.

2. Gravitational radiation spins the star down at a rate $-\dot{J}_{\rm GR} = 6MR^2\Omega\gamma_{GR}|C_R|^2$. If $-\dot{J}_{\rm GR} < \dot{J}_{acc}$, the star spins up until $\dot{J}_{\rm GR} = -\dot{J}_{acc}$. Otherwise, if $-\dot{J}_{GR} > \dot{J}_{acc}$, the star will spin down and reenter the region in which the R-mode is stable. In spin equilibrium, $J = I\Omega_{eq} \propto IM^{5/7}\mu^{-6/7}$,

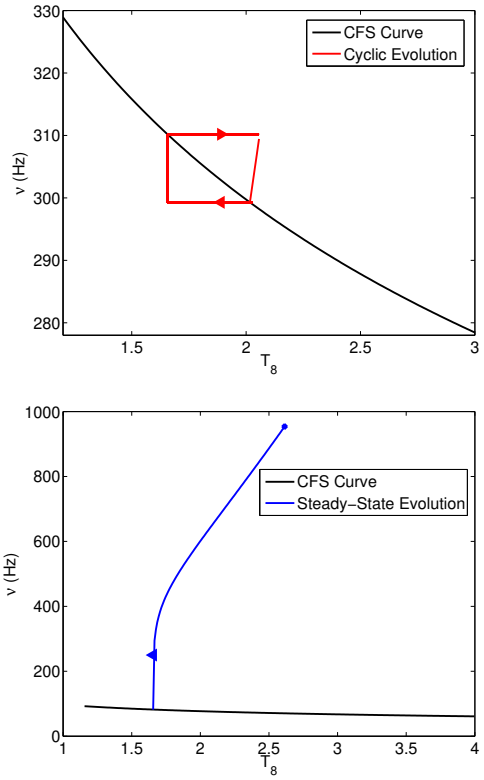

FIG. 1.—: Schematic $\nu - T$ evolutions are shown when the dissipation is dominated by (a) boundary layer viscosity (b) shear viscosity. It can be seen that in the latter case the star spins to much higher frequencies. The final spin frequency where the accretion torque is balanced by gravitational emission is given by Eq.(19). The CFS instability curve occurs when the gravitational driving equals the viscous damping of the R-mode.

where $\Omega_{eq} = 2\pi\nu_{eq}$ and ν_{eq} is given by Eq. 1. As accretion proceeds, the magnetic moment decreases and ν_{eq} increases (e.g. Shibazaki et al. 1989; Zhang & Kojima 2006). A good approximation is $\mu \propto (\Delta M)^{-\beta}$, where ΔM is the total mass accreted, and so $J \propto IM^{5/7}(\Delta M)^{6\beta/7}$; Shibazaki et al. (1989) originally suggested $\beta = 1$, but Zhang & Kojima (2006) advocate $\beta = 7/4$ until μ "bottoms out" at $\mu_{26} \simeq 1$ (see also Wang et al. 2011). In general, the accretion torque is defined to be $\dot{J}_{acc} = \dot{M}dJ/dM$, which can be written as $\dot{J}_{acc}/J = \sigma_J \dot{M}/M$, where $\sigma_J = 6\beta M/7\Delta M + 5/7 + d\ln I/d\ln M$; spin up is faster before μ bottoms out and $\beta \to 0$ and slows as mass accretes and ν increases. As a simple model, we adopt $\dot{J}_{acc}/J = \gamma_{\rm acc}(\nu_0/\nu)^{2s}$; for numerical estimates, we take $\gamma_{\rm acc}(\nu_0/\nu)^{2s} = 10^{-8}\,{\rm y}^{-1}\,\gamma_{{\rm acc},8}\nu_{500}^{-2s}$, where $s \approx 1/3$ and $s \approx 0.7$ respectively before and after μ bottoms out. The parameter $\gamma_{{\rm acc},8}$ is different for each accreting neutron star. With this simplified model, $\dot{J}_{\rm GR} = -\dot{J}_{acc}$ at an R mode amplitude

$$|C_R|_j \approx \frac{2.1\times10^{-7}(\mathcal{I}_{0.3}\gamma_{{\rm acc},8})^{1/2}}{\nu_{500}^{3+s}M_{1.4}^{1/2}R_{10}^2}\ , \qquad (7)$$

where the moment of inertia of the star is $I = 0.3\mathcal{I}_{0.3}MR^2$. For numerical estimates, we shall use $s = 1/3$, since most of the spin up occurs in this regime. Comparing Eq. (7) with Eq. (7) we see that $|C_R|_j \lesssim 0.1|C_R|_{\rm PIT}$, which means that $\dot{J}_{GR} > -\dot{J}_{acc}$, and spin up is prevented.

3. The amplitude at which heating by the R mode balances heating via accretion, $H_{acc} = \epsilon_{acc}\dot{M}c^2$ with $\epsilon_{acc} = 10^{-3}\epsilon_{acc,3}$ (Brown 2000), is

$$|C_R|_H \approx \frac{5.5\times10^{-8}(\epsilon_{acc,3}\dot{M}_9)^{1/2}}{\nu_{500}^4M_{1.4}R_{10}^3}\ . \qquad (8)$$

For $|C_R|_{\rm PIT} > |C_R|_H$, heating by the R mode dominates. Comparing Eq. (8) with Eq. (7) implies that heating by the R mode is more important than accretional heating for damping in a shearing boundary layer.

4. A fourth important amplitude comes from equating gravitational radiation spindown with $-\dot{J}_B = \eta_{\rm mag}\mu^2\Omega^3/3c^3$, the rate of pulsar spindown,

$$|C_R|_B \approx \frac{1.5\times10^{-8}\mu_{26}\eta_{\rm mag}^{1/2}}{\nu_{500}^2M_{1.4}R_{10}^3}\ . \qquad (9)$$

This is relevant to the evolution after accretion ceases. If $|C_R|_{\rm PIT} > |C_R|_B$ then spindown via gravitational radiation is faster than pulsar spindown.

For damping in a shearing boundary layer, $|C_R|_{\rm PIT} > |C_R|_j$ and so accretion spin-up is limited to about 300 Hz, which is inconsistent with observations of pulsars spinning up to 716 Hz. In Fig. 1, the left panel illustrates a typical evolution sequence in this case. Because $|C_R|_{\rm PIT} > |C_R|_j$, the evolutionary track in the $\nu - T$ plane is a rather tight cycle that is confined to a small range of frequencies $\leq \nu_S$, the frequency at which the mode first becomes unstable, given in Eq. (4).

For spin up substantially beyond 300 Hz to be possible, $|C_R|_{\rm PIT}$ must remain below $|C_R|_j$ up to frequencies well above ν_S. Eq. (7) shows that $|C_R|_{\rm PIT} \gtrsim 3\gamma_D/2\kappa_D\Omega$, but that for damping within a viscous shearing boundary layer γ_D is too large to allow significant spin up. However, Eq. (7) also suggests that *lower* γ_D would permit prolonged spin up. In §3 we examine what happens if a thin viscous shearing boundary layer does not form near the core-crust boundary, so that γ_D is due to shear viscosity damping distributed over the entire star. In Fig. 1, the right panel illustrates the sort of evolution that would become possible in this case. As can be seen from the figure, prolonged spin up is possible, but even in this case there is a maximum attainable spin frequency. We conjecture – but do not prove —that if the transition from core (super)fluid to crustal solid is gradual enough, a thin viscous shearing boundary layer does not form.

After accretion ceases, $|C_R|_{\rm PIT}$ must be small enough that gravitational radiation spin down timescales are $\gtrsim 10^9$ years in order for fast spin to be maintained on spin down timescales characteristic of the fastest millisecond pulsars. Otherwise, the spun up neutron star would simply spin down too rapidly via gravitational radiation, roughly retracing its steps down to the stable region, leaving a millisecond pulsar with spin frequency $\nu_S \simeq 300\,{\rm Hz}$. Under these circumstances, heating due to the R mode will be less important than in Bondarescu et al. (2007) during spin up, but may still dominate over accretional heating. If these conditions can be met, the star heats modestly after becoming unstable, but continues to spin up by a significant factor. After accretion stops, the star cools and spins down within the unstable regime, but $|C_R|_{\rm PIT}$ is too small to accelerate spin down substantially, and the spun-up neutron star can become a long-lived millisecond pulsar. Such a scenario is unfavorable for gravitational radiation detection, but essential for understanding how pulsars spin up to frequencies $\gtrsim 500$ Hz.

3. CONDITIONS FOR A SUCCESSFUL OUTCOME OF SPIN-UP

In §2 we demonstrated that the R mode instability frustrates prolonged spin-up *if* dissipation is due to a viscous shearing boundary layer at the boundary between the stellar core and crust. The left panel of Fig. 1 illustrates the problem graphically. If, for some reason, such a thin viscous boundary layer does not arise, then damping would be due to shear viscosity damping distributed over the entire star. This would result in lower damping rates, and lower $|C_R|_{\rm PIT} \gtrsim 3\gamma_D/2\kappa_D\Omega$.

We conjecture that if the transition from fluid core to solid crust occurs over a radial zone that is considerably thicker than the boundary layer size, $\ell \simeq (\eta/\Omega)^{1/2} \simeq 1.8K_4^{1/2}\nu_{500}^{-1/2}T_8^{-1}$ cm, then a thin viscous boundary layer will not form. In passing from the fluid core to the solid crust, a mode experiences a velocity jump Δv. If the transition from core to crust is abrupt, then the jump is disontinuous in the inviscid limit. Viscous effects smooth the jump so that it occurs continuously; the smoothing length is ℓ which is very small but not zero. Dissipation within this layer is vigorous, with $\dot{E} \simeq 4\pi\rho_b r_b^2\ell(\Delta v)^2 \times$

$\eta/\ell^2 \propto \ell^{-1}$.

Suppose that instead of an abrupt transition, the shear modulus of the star grows from zero near r_b to its value at the inner edge of the crust over a radial zone of thickness $\Delta r \gg \ell$. Then we expect the velocity jump to occur over this relatively extended region. We do not present a rigorous calculation of how this happens, since there are many uncertainties, principally in how the shear modulus grows within the transition region. The crude toy model developed in Appendix B illustrates the salient features. Fig. 2 shows how the displacement field evolves smoothly across the layer in this toy model. The dissipation associated with this smooth transition is $\dot{E} \sim 4\pi r_b^2 \Delta r (\Delta v)^2/ \times \eta/(\Delta r)^2 \propto (\Delta r)^{-1}$. (For the specific case of the toy model computed in Appendix B the constant of proportionality is about two.) For $\Delta r \gg \ell$, the dissipation rate associated with a smooth transition layer is much smaller than the dissipation rate that would arise in a thin boundary layer. For moderate velocity jumps, such as the relatively small jump associated with the R mode, the extended transition layer contributes relatively little compared with the energy dissipation associated with shear viscosity across the entire star.

In the remainder of this section, we assume that dissipation is due to the distributed effect of shear viscosity. We consider two cases: a "permeable" limit where the daughter modes penetrate into the crust, and an "impermeable" limit where they do not. We estimate the *lowest value* of $|C_R|_{\rm PIT}$ for each of these cases, taking full account of the two factors in Eq. (5). In order to get an estimate, we need scaling relations for κ_D, $\delta\omega$ and γ_D with n_D. As was mentioned above, explicit calculations by Brink et al. (2004) (see also Brink 2005) indicate that κ_D does not rise systematically with n_D, the principal mode number of the daughters, although larger values become likelier as n_D increases. We use statistical arguments for the expected smallest value of $\delta\omega$ as a function of n_D. We use WKB calculations presented in §A.5 plus explicit numerical evaluations (Brink et al. 2004; Brink 2005) for γ_D. The upshot is that $\delta\omega$ tends to decrease with n_D whereas γ_D tends to increase, so there is a minimum value of $|C_R|_{\rm PIT}$ at large values of n_D. We shall demonstrate that the minimum occurs at $n_D \simeq 100$, considerably beyond the ranges computed explicitly even for the modes of an incompressible star.

3.1. *Permeable Crust*

Let us consider the non-rigid case first. The WKB calculation detailed in Appendix A.5 implies that

$$\gamma_D \simeq \frac{p_D^2(\eta_{core}-\eta_{crust})(r_b/R)^2}{R^2\sqrt{1-(r_b/R)^2}} + \frac{2p_D^3\eta_{crust}}{3R^2} \qquad (10)$$

assuming different kinematic viscosities η_{core} and η_{crust} in the core ($r \le r_b$) and crust ($r_b < r \le 1$), respectively; here $p_D = \sqrt{n_D(n_D+1) - |m_D|(|m_D|+1)} \simeq n_D$. The second term dominates for sufficiently large values of n_D, but since $\eta_{crust} \ll \eta_{core}$ (Shternin & Yakovlev 2008) for practical purposes almost all of the dissipation occurs in the core. (For uniform $\eta_{core} = \eta_{crust}$ the second term dominates, and Eq. (10) agrees with results in Brink et al. (2004).) Moreover, comparing Eqs. (B7) and (10), with $\eta_b \sim \eta_{core}$, we see that dissipation in the bulk of the star dominates over dissipation in the transition region as long as $p_D \simeq n_D \gtrsim S_D\sqrt{R/\Delta R} = 10 S_D\sqrt{R/100\Delta R_t}$. Tentatively, we assume that this inequality holds for the daughter modes involved in the lowest $|C_R|_{\rm PIT}$; we shall see that this is likely to be true. Thus we adopt $\gamma_D = \gamma_0 n_D^2$ for estimating the lowest $|C_R|_{\rm PIT}$; from the first term in Eq. (10) with $p_D \simeq n_D$ (as WKB requires)

$$\frac{\gamma_0}{\Omega} = \frac{\eta_{core}(r_b/R)^2}{\Omega R^2\sqrt{1-(r_b/R)^2}} = \frac{5.9\times10^{-12}K_4}{\nu_{500}T_8^2R_{10}^2} \qquad (11)$$

where $\eta_{core} = 10^4 K_4 T_8^{-2}\,{\rm cm^2\,s^{-1}} = \eta_b$ and we set $r_b = 0.9R$.

The other factor in Eq. (5) is the detuning. The *minimum* $\delta\omega/\Omega$ up to principal quantum number n is *expected* to be approximately $2\sqrt{2}/N(<n)$, where $N(<n) \approx \frac{1}{6}n^4$ is the number of couplings to the R mode consistent with selection rules for the transitions (Brink 2005). Since we are seeking an estimate of the lowest $|C_R|_{\rm PIT}$ we substitute this into Eq. (5) to get

$$|C_R|^2_{\rm PIT} = \frac{9}{4\kappa_D^2}\left(\frac{\gamma_0^2 n_D^4}{\Omega^2} + \frac{72}{n_D^8}\right)\ ; \qquad (12)$$

recalling that κ_D is relatively insensitive to n_D we minimize the quantity in brackets over n_D and find the lowest value of the threshold at

$$n_D = 1.5\left(\frac{\Omega}{\gamma_0}\right)^{1/6} \approx \frac{110\nu_{500}^{1/6}T_8^{1/3}R_{10}^{1/3}}{K_4^{1/6}} \qquad (13)$$

where we have used $r_b = 0.9R$, and therefore

$$|C_R|_{\rm PIT,min} = \frac{4.2}{\kappa_D}\left(\frac{\gamma_0}{\Omega}\right)^{2/3} \approx \frac{1.4\times10^{-7}K_4^{2/3}}{\kappa_D\nu_{500}^{2/3}T_8^{4/3}R_{10}^{4/3}}\ . \qquad (14)$$

Requiring that $|C_R|_{\rm PIT} < |C_R|_j$ implies that nonlinear dynamics limits spin up to frequencies

$$\nu \lesssim \frac{590\,{\rm Hz}\,\kappa_D^{3/8}T_8^{1/2}(\mathcal{I}_{0.3}\gamma_{\rm acc,8})^{3/16}}{K_4^{1/4}M_{1.4}^{3/16}R_{10}^{1/4}}\ , \qquad (15)$$

where we have used $s = 1/3$ to obtain the numerical value. The existence of a maximum spin frequency limit for spin up via accretion is a generic feature of the dynamics: $|C_R|_{\rm PIT,min}$ is determined by a competition between the decrease of the smallest expected detuning $\delta\omega$ and the increase of the dissipation γ_D with increasing n_D.

Including other physical features that we have neglected here will not do away with this key feature of the dynamics. Two physical features we shall study subsequently are buoyancy and relativistic corrections. Buoyancy shifts mode frequencies, but *not* that of the R mode (Saio 1982; Yoshida & Lee 2000a), and also activates the $n \ne |m|+1$ r modes in the star (Saio 1982; Yoshida & Lee 2000b). Relativistic corrections also shift mode frequencies (e.g. Lockitch et al. 2000, 2003), and may also generate non-axial contributions to the R mode eigenfunction that permit additional couplings that would be forbidden non-relativistically (see e.g. Lockitch et al. 2000, 2003). Studies that combine buoyancy and relativity are tricky (Kojima 1998; Kojima & Hosonuma 1999; Boutloukos & Nollert 2007; Passamonti et al. 2008, e.g.)

but detailed calculations seem to support the existence of a mode structure very similar to the Newtonian case (Lockitch et al. 2004, 2001; Lockitch et al. 2003; Pons et al. 2005; Villain et al. 2005). In any event, including both buoyancy and relativistic corrections will not alter the key feature of the network of interacting modes, namely that there exists a dense set of frequencies bounded above and below, which permits an increasing number of near resonances as n_D increases. Moreover, additional couplings may become possible that would be forbidden otherwise, which could lower the value of $|C_R|_{\rm PIT,min}$, thus permitting spin up to larger ν. Differential rotation and magnetic fields (Rezania & Morsink 2002; Rezzolla et al. 2000, 2001a,b) and mutual friction (Haskell et al. 2013) may play an important role in limiting the R-mode amplitude. More work is needed to investigate such effects in detail.

The existence of a maximum frequency dictated by the nonlinear dynamics is a basic conclusion of this paper. The actual value of the maximum frequency depends on the external variable, $\gamma_{\rm acc,8}$, even though the dependence is weak. Each individual neutron star has its own value of $\gamma_{\rm acc,8}$, so the maximum spin rate that is attainable is *not* the same for all neutron stars. We emphasize that our estimate of $|C_R|_{\rm PIT,min}$ is the key to determining the value of the maximum spin reate. The saturation amplitude of the R mode is not an adjustable parameter, but is determined by the nonlinear hydrodynamics of the network of interacting modes.

It is reassuring that the value of the maximum frequency in Eq. (15) is close to 700 Hz, but to go further we need the value of T_8 in particular; this is determined from balancing heating and neutrino cooling. We determine T from the relationship

$$L_\nu = H_{acc} + H_R, \tag{16}$$

where L_ν is the neutrino cooling rate. We assume that cooling is primarily via the Cooper pair process, with $L_\nu \simeq 10^{33} f_\nu T_8^8\,{\rm ergs}^{-1}$ where $f_\nu \sim 1$ may depend on M and R (e.g. Gusakov et al. 2004; Page et al. 2004, 2011; Shternin et al. 2011). We evaluate H_R using $|C_R|_{\rm PIT,min}$ from Eq. (14); with $H_R = \epsilon_{acc}\dot{M}c^2$ we find that thermal balance implies

$$f_\nu T_8^8 = 57\dot{M}_9\epsilon_{acc,3} + \frac{360\nu_{500}^{20/3}K_4^{4/3}M_{1.4}^2R_{10}^{10/3}}{\kappa_D^2 T_8^{8/3}}\ , \tag{17}$$

which defines a curve in the $\nu - T$ plane along which the star evolves during acrretion. Eq. (17) shows that H_{acc} dominates at low ν_{500} (e.g. where the instability ensues), and $T_8 \approx 1.7(\dot{M}_9\epsilon_{acc,3}/f_\nu)^{1/8}$ in this regime; H_R dominates at large ν_{500} (i.e. where the upper spin limit is fixed) and

$$T_8 \approx \frac{1.7\nu_{500}^{5/8}K_4^{1/8}M_{1.4}^{3/16}R_{10}^{5/16}}{\kappa_D^{3/16}f_\nu^{3/32}}\ . \tag{18}$$

Using Eq. (18) in Eq. (15) implies a more precise upper bound

$$\nu \lesssim \frac{950\,{\rm Hz}\,\kappa_D^{9/22}(\mathcal{I}_{0.3}\gamma_{\rm acc,8})^{3/11}}{f_\nu^{3/44}K_4^{3/11}(M_{1.4}R_{10})^{3/22}} \equiv \nu_{max}\ . \tag{19}$$

The full solution of Eq. (17) would give a slightly lower value.

Because γ_D is low, spin up begins at a significantly lower frequency than Eq. (4), typically $\nu_S \simeq 100 - 150\,{\rm Hz}$, so prolonged spin up via accretion is required. Throughout much of this evolution, the R mode plays almost no role because of the strong frequency dependences of H_R/H_{acc} and $|C_R|_{\rm PIT,min}/|C_R|_j$. Spin up ends either because accretion ceases or because spin equilibrium $|C_R|_{\rm PIT} = |C_R|_j$ is achieved. In the former case, spin up proceeds almost as it would if there were no R mode instability. At its maximum spin frequency, a neutron star is in spin balance, with equal and opposite gravitational radiation and accretion torques, and remains in that state until accretion ends. Depending on the detailed evolution, spin equilibrium can occupy a substantial fraction of the time during which a neutron star accretes. In thermal balance, Eq. (17) shows that the neutron star's internal temperature is an increasing function of frequency, but also depends on $\dot{M}_9$, which is different for each accreting neutron star, and κ_D. Although we expect *similar* values of κ_D for different neutron stars, they need not be *identical*, because n_D is not the same for all neutron stars affected by the R mode instability. Thus, there may be some variability in internal and effective temperatures for neutron stars in the unstable domain. Intermittent accretion is unlikely to affect these conclusions: cooling timescales are $\sim 100 - 1000$ years so if the heating rate fluctuates at much shorter timescales the time averaged heating rate is all that matters. Similarly, the detailed time dependent dynamical evolution of the R mode proceeds on timescales that are too short, $\sim 1/\delta\omega \sim 1/|C_R|_{\rm PIT}\Omega$, to be important for the secular evolution of spin and internal temperature; whether there are any observable effects of the dynamics is beyond the scope of this paper.

Once accretion ends, the fast rotating neutron star cools and spins down. Because the cooling timescale is short compared with the spin down timescale ($\gtrsim 10^8\gamma_{\rm acc,8}^{-1}$ years) at the end of spin up, the neutron star first cools at fixed spin frequency. Cooling ends when H_R is balanced by cooling. Once this point is reached, the neutron star spins down along the curve given by Eq. (18), and

$$|C_R|_{\rm PIT,min} \approx \frac{6.6\times10^{-8}K_4^{1/2}f_\nu^{1/8}}{\nu_{500}^{3/2}\kappa_D^{3/4}M_{1.4}^{1/4}R_{10}^{7/4}}\ . \tag{20}$$

Slow evolution along this curve is driven by spin down: if there were no change in ν the star would remain at a single point in the $\nu - T$ plane. The total spin down rate is the sum of contributions from gravitational radiation and electromagnetic radiation $-\dot{J} = \dot{J}_{GR} + \dot{J}_B$. The spin-down rate at the lowest PIT given by Eq. (20) is

$$-\frac{\dot{J}}{I\Omega} \approx \frac{(\nu/\nu_{max})^{11/3}\gamma_{\rm acc,8}}{10^8\,{\rm y}\,\nu_{max,500}^{2/3}} + \frac{\eta_{\rm mag}\mu_{26}^2\nu_{500}^2}{14.5\times10^9\,{\rm y}\,\mathcal{I}_{0.3}M_{1.4}R_{10}^2}\ , \tag{21}$$

where we have used $\nu_{max,500} = \nu_{max}/500\,{\rm Hz}$. Spin down ages $t_{sd} = -I\Omega/2\dot{J}$ for radiopulsars with $\nu \gtrsim 400\,{\rm Hz}$ range between 1.64×10^8 y and 14.3×10^{10} y; see Manchester et al. (2005),

http://www.atnf.csiro.au/research/pulsar/psrcat/. If we require a spindown age $\gtrsim 10^9$ years at ν_{max}, Eq. (21) implies that $\gamma_{\rm acc,8} \lesssim 0.05$. Inserting this into Eq. (19) lowers ν_{max}, keeping all other parameters fixed. Since $\nu_{max} \propto (\kappa_D \gamma_{\rm acc,8}^{2/3}/K_4^{2/3})^{9/22}$, the bound can still be around 750 Hz if $\kappa_D/K_4^{2/3} \gtrsim 4.1$; values of κ_D this large are unusual but not unheard of for incompressible stars (Brink et al. 2004; Brink 2005), and it is conceivable that $K_4 \lesssim 1$. This scenario for millisecond pulsar formation requires that *all* of the fastest spinning pulsars are in the *unstable* domain. Eq. (21) predicts spin down indices $n = \nu\ddot{\nu}/\dot{\nu}^2 > 3$. Determinations of $\ddot{\nu}$ for millisecond pulsars are contaminated by timing noise so there is no conclusive evidence against this picture.

3.2. *Impermeable Crust*

Calculations for the rigid case follow closely the methodology of §3.1 but there is an important difference: because the daughter modes are confined to the core, for practical purposes R is replaced by r_b in the WKB solutions. We regard this as an extreme limit, and that more realistically, for the values of n_D we estimate below, the daughter modes penetrate the crust incompletely with a fractional velocity jump $S_D \lesssim 1$. In this case, we get a damping rate

$$\gamma_D = \frac{2p_D^3 \eta_{core}}{3r_b^2} \tag{22}$$

i.e. we get the second term in Eq. (10) with $R \to r_b$ and $\eta_{crust} \to \eta_{core}$. There is no need to include the effect of the transition region, since it is already included (and partly responsible for the stronger scaling with p_D). Instead of Eq. (12) we get

$$|C_R|^2_{\rm PIT} = \frac{9}{4\kappa_D^2}\left(\frac{\gamma_0^2 n_D^6}{\Omega^2} + \frac{72}{n_D^8}\right) \tag{23}$$

but with (letting $r_b = 9r_{b,9}$ km)

$$\frac{\gamma_0}{\Omega} = \frac{\eta_{core}}{3\Omega r_b^2} = \frac{2.6\times 10^{-12} K_4}{\nu_{500} T_8^2 r_{b,9}^2}\ . \tag{24}$$

Neglecting variations in κ_D as before, Eq. (23) is minimize at

$$n_D = 1.4\left(\frac{\Omega}{\gamma_0}\right)^{1/7} \approx \frac{63\nu_{500}^{1/7} T_8^{2/7} r_{b,9}^{2/7}}{K_4^{1/7}} \tag{25}$$

and

$$|C_R|_{\rm PIT,min} = \frac{5.3}{\kappa_D}\left(\frac{\gamma_0}{\Omega}\right)^{4/7} \tag{26}$$

Following the same procedure as led to Eqs. (19) and (20) leads to the final results

$$\nu \lesssim \frac{360\,{\rm Hz}\,\kappa_D^{7/18}(\mathcal{I}_{0.3}\gamma_{\rm acc,8})^{1/4} r_{b,9}^{4/9}}{K_4^{2/9} f_\nu^{1/18} M_{1.4}^{5/36} R_{10}^{2/3}} \equiv \nu_{max} \tag{27}$$

and

$$|C_R|_{\rm PIT,min} \approx \frac{4.1\times 10^{-7} K_4^{4/9} f_\nu^{1/9}}{\nu_{500}^{4/3}\kappa_D^{7/9} M_{1.4}^{2/9} R_{10}^{2/3} r_{b,9}^{8/9}}\ . \tag{28}$$

Eq. (27) requires $\kappa_D \gamma_{\rm acc,8}^{9/14}/K_4^{4/7} \gtrsim 6.6$ for $\nu_{max} \approx 750\,{\rm Hz}$, holding all other paramters fixed. Eq. (28) implies a spin down rate

$$-\frac{\dot{J}}{I\Omega} \approx \frac{(\nu/\nu_{max})^4 \gamma_{\rm acc,8}}{10^8\,{\rm y}\,\nu_{max,500}^{2/3}} + \frac{\eta_{\rm mag}\mu_{26}^2\nu_{500}^2}{14.5\times 10^9\,{\rm y}\,\mathcal{I}_{0.3}M_{1.4}R_{10}^2}\ . \tag{29}$$

Just as we found for the nonrigid case, we need to cut down the gravitational radiation contribution in order to be consistent with pulsar data: requiring a spin down timescale due to gravitational radiation $\gtrsim 10^9$ years near ν_{max} implies $\gamma_{\rm acc,8} \lesssim 0.05$, and for $\nu_{max} \simeq 750\,{\rm Hz}$ we would then require $\kappa_D/K_4^{4/7} \gtrsim 45$, which is a more stringent constraint than we found in §3.1.

4. CONCLUSIONS

Our examination of the nonlinear dynamics of rotational modes of a neutron star suggests that in the conventional picture, where modes damp in a thin viscous boundary layer, spin up beyond about 300 Hz is not possible: not only is the frequency at which the R mode first destabilizes about 300 Hz (see Eq. (4)) but the R mode amplitude saturates at a level large enough that gravitational radiation spindown prevents significant spin up subsequently (see Eq. (7)). Thus, we consider what happens if a thin shearing boundary layer cannot form. We conjecture that this may happen if the transition between core and crust occurs in a region thicker than $\sim 1-2$ cm, and justify that assumption partially with the toy model in Appendix B. If a thin boundary layer does not form, damping of all modes is dominated by the distributed effects of shear viscosity throughout the star, which leads naturally to a lower R mode saturation amplitude.

Using scaling relations found by a combination of exact calculations for incompressible stars (Brink et al. 2004; Brink 2005), statistical arguments (Brink 2005) and approximate WKB calculations (Appendix A) we estimate the lowest parametric instability threshold $|C_R|_{\rm PIT,min}$ analytically for coupling of the R mode to pairs of daughters. We find that the daughter modes for which this occurs are at principal mode quantum $n_D \simeq 100$, typically; this is beyond the range for which explicit calculations exist, even for incompressible stars. We stress that the lowest parametric instability threshold sets the amplitude at which the R mode amplitude saturates during evolution of a network of rotational modes of a neutron star (Brink et al. 2005). Thus, our estimate of $|C_R|_{\rm PIT}$ represents a first principles calculation of the saturation amplitude. We stress that this is *not* an adjustable parameter, but rather arises from the nonlinear hydrodynamics. Although it may seem counterintuitive, when there are many nearly resonant modes, as is the case for a rotating neutron star, nonlinear effects become important at low amplitude, and lead to saturation.

With the lower $|C_R|_{\rm PIT,min}$ that arises when shear viscosity dominates the damping, prolonged spin up to frequencies above 500 Hz is possible. A basic conclusion is that the nonlinear development of the R mode instability naturally gives rise to an upper spin frequency limit. This bound arises from the requirement that $|C_R|_{\rm PIT,min}$ be smaller than $|C_R|_j$, the amplitude where gravitational radiation spin down balances accretion spin up. Eq. (19) and Eq. (27) provide rough estimates for the maximum

spin frequency ν_{max} that can be attained under the assumption that the crust is permeable and impermeable to small scale modes, respectively. It is plausible that $\nu_{max} \simeq 750\,\mathrm{Hz}$, but consistency with observations of millisecond pulsars requires relatively strong (but not outrageously strong) coupling κ_D; smaller values are allowed for the permeable case, which may argue in its favor. This suggests that nonlinear interactions among the rotational modes of a neutron star may naturally imply a maximum spin frequency below what one might expect from dynamical instabilities of the star. This conclusion is compatible with studies that suggest that LMXBs are not spun up beyond about 730 Hz (Chakrabarty 2005, 2008, 2012) as well as the fact that the fastest spinning neutron star yet discovered spins at 716 Hz.

A second conclusion of our study is that after accretion ceases, fast spinning millisecond pulsars cool until they reach a balance between neutrino cooling and heating that results from the energy sent to smaller scale modes from the unstable R mode. The result is slow evolution along a curve in the $\nu - T$ plane, Eq. (18). Spindown timescales are sufficiently long that once spun up a millisecond pulsar ought to remain close to the upper part of this curve. This means that millisecond pulsars remain stuck in the domain where the R mode is unstable, and are therefore radiating gravitational radiation. However, the emission rate is very low, and strain amplitudes at Earth are correspondingly low, $\sim 10^{-26}/D_{kpc}t_{sd,9}$ for a source at $D = D_{kpc}$ kpc with a spin down time $10^9 t_{sd,9}$ years. Although gravitational radiation may dominate the spin down, because the accretion spin up rate generally sets torque amplitudes we expect millisecond pulsars to be near the conventional spin up line but possibly slightly above it.

APPENDIX

ASSORTED WKB RESULTS

Preliminaries: Coordinates

The Bryan coordinates $x_{1,2}$: for a mode with $\omega = 2\Omega|\mu| \equiv 2\Omega\cos\theta_{|\mu|} \leq 2\Omega$ are

$$\begin{aligned}
\varpi &= \sqrt{x^2+y^2} = \sqrt{\frac{(1-x_1^2)(1-x_2^2)}{1-\mu^2}} = \frac{\sin\theta_1\sin\theta_2}{\sqrt{1-\mu^2}} \\
z &= \frac{x_1 x_2}{|\mu|} = \frac{\cos\theta_1\cos\theta_2}{|\mu|} \\
x_1 &\in [|\mu|,1] \quad x_2 \in [-|\mu|,|\mu|] \\
\theta_1 &\equiv \cos^{-1}(x_1) \in [0,\theta_{|\mu|}] \quad \theta_2 \equiv \cos^{-1}(x_2) \in [\theta_{|\mu|},\pi-\theta_{|\mu|}] \ .
\end{aligned} \tag{A1}$$

We use units in which the radius of the star is $R = 1$. The following are useful definitions: with $\theta_\pm = \theta \pm \theta_{|\mu|}$

$$\begin{aligned}
\cos(\theta_2-\theta_1) &= z|\mu| + \varpi\sqrt{1-\mu^2} = r\cos\theta_- \\
\cos(\theta_2+\theta_1) &= z|\mu| - \varpi\sqrt{1-\mu^2} = r\cos\theta_+ \ .
\end{aligned} \tag{A2}$$

For finding mode displacements, we will want derivatives of $\theta_{1\,\mathrm{or}\,2}$ with respect to coordinates. In cylindrical coordinates Eq. (A1) implies

$$\begin{aligned}
\sqrt{1-\mu^2}\,d\varpi &= \cos\theta_1\sin\theta_2 d\theta_1 + \sin\theta_1\cos\theta_2 d\theta_2 \\
|\mu|\,dz &= -\sin\theta_1\cos\theta_2 d\theta_1 - \cos\theta_1\sin\theta_2 d\theta_2 \\
d\theta_1 &= \frac{\cos\theta_1\sin\theta_2 d\varpi\sqrt{1-\mu^2} + \sin\theta_1\cos\theta_2 dz|\mu|}{\cos^2\theta_1\sin^2\theta_2 - \sin^2\theta_1\cos^2\theta_2} \\
d\theta_2 &= \frac{\cos\theta_2\sin\theta_1 d\varpi\sqrt{1-\mu^2} + \sin\theta_2\cos\theta_1 dz|\mu|}{\cos^2\theta_2\sin^2\theta_1 - \sin^2\theta_2\cos^2\theta_1}
\end{aligned} \tag{A3}$$

Using Eqs. (A3) we find the area element

$$dA = \varpi d\varpi dz = \frac{\sin\theta_1\sin\theta_2(\cos\theta_1^2 - \cos\theta_2^2)d\theta_1 d\theta_2}{|\mu|(1-\mu^2)} = \frac{(x_1^2-x_2^2)dx_1 dx_2}{|\mu|(1-\mu^2)} \ . \tag{A4}$$

(The integral $\int dA$ over the ranges of $\theta_{1,2}$ or $x_{1,2}$ is 2/3.) The stellar surface $r = 1$ is patched together in the following way:

$$\begin{aligned}
&\theta_1 = \theta_{|\mu|} \quad \text{and} \quad \theta_2 = \theta \in [\theta_{|\mu|},\pi-\theta_{|\mu|}] \\
&\theta_2 = \theta_{|\mu|} \quad \text{and} \quad \theta_1 = \theta \in [0,\theta_{|\mu|}] \\
&\theta_2 = \pi-\theta_{|\mu|} \quad \text{and} \quad \theta_1 = \pi-\theta \in [0,\theta_{|\mu|}] \ .
\end{aligned} \tag{A5}$$

There are special points where $x_1^2 - x_2^2 = 0 = dA$; at these points, $\cos\theta_1 = \pm\cos\theta_2 = |\mu|$.

WKB Approximation to Displacements

From Arras et al. (2003) §3.2 we take the WKB Eulerian enthalpy perturbation to be [2]

$$\Psi \approx \frac{P_{nm}(x_1)P_{nm}(x_2)\exp[i(m\phi+\omega t)]}{\sqrt{\rho}} \approx \frac{\cos(p\theta_1+\alpha_1)\cos(p\theta_2+\alpha_1)\exp[i(m\phi+\omega t)]}{\sqrt{\rho\sin\theta_1\sin\theta_2}} \tag{A6}$$

where $\rho=\rho(r)$ is the density profile and $p=\sqrt{n(n+1)-m(m+1)}\simeq n$. The first approximation assumes that the density scale height is large compared with characteristic scales on which Ψ varies. The second approximation is for the associated Legendre functions, and holds at sufficiently large values of p. The values of the phases α_i depend on the parity of the mode: based on asymptotic properties of the $P_{nm}(z)$, Arras et al. (2003) adopted $\alpha_1=\alpha_2=-p\pi/2$ or $=-(p+1)\pi/2$ even or odd parity, respectively, but Ivanov & Papaloizou (2010), using a more delicate treatment of boundary conditions, argued for $\alpha_1\neq\alpha_2$. The exact phases should not matter for computing most quantities and we adopt the values used by Arras et al. (2003).

Mode displacements are computed from the equation [3]

$$\left(1-\frac{1}{\mu^2}\right)\boldsymbol{\xi} = \boldsymbol{\nabla}\Psi - \frac{\hat{\boldsymbol{z}}\hat{\boldsymbol{z}}\cdot\boldsymbol{\nabla}\Psi}{\mu^2} + \frac{i\hat{\boldsymbol{z}}\times\boldsymbol{\nabla}\Psi}{\mu} \tag{A7}$$

up to an overall normalization factor. With the approximation that the density scale height is large, we do not include derivatives of ρ in computing the displacements; thus we write

$$\begin{aligned}\sqrt{\rho}\left(1-\frac{1}{\mu^2}\right)\boldsymbol{\xi} \approx \exp(+i\omega t)\Bigg\{ & \boldsymbol{\nabla}\left[P_{nm}(x_1)P_{nm}(x_2)\exp(im\phi)\right] \\ & -\frac{\hat{\boldsymbol{z}}\hat{\boldsymbol{z}}\cdot\boldsymbol{\nabla}\left[P_{nm}(x_1)P_{nm}(x_2)\exp(im\phi)\right]}{\mu^2} \\ & +\frac{i\hat{\boldsymbol{z}}}{\mu}\times\boldsymbol{\nabla}\left[P_{nm}(x_1)P_{nm}(x_2)\exp(im\phi)\right]\Bigg\} .\end{aligned} \tag{A8}$$

For evaluating the derivatives, we use

$$\begin{aligned}\boldsymbol{\nabla}P_{nm}(x_i) &= \frac{dP_{nm}}{dx_i}\boldsymbol{\nabla}x_i \\ \boldsymbol{\nabla}x_i &= -\sin\theta_i\boldsymbol{\nabla}\theta_i = -\sqrt{1-x_i^2}\boldsymbol{\nabla}\theta_i\end{aligned} \tag{A9}$$

where the $\boldsymbol{\nabla}\theta_i$ were computed in Eqs. (A3). If we further invoke the large p approximation to the associated Legendre polynomials, then we ignore the variation of the $\sin\theta_i$ factors in computing derivatives; in this approximation

$$\begin{aligned}\sqrt{\rho\sin\theta_1\sin\theta_2}\left(1-\frac{1}{\mu^2}\right)\boldsymbol{\xi} \approx \exp(+i\omega t)\Bigg\{ & \boldsymbol{\nabla}\left[\cos(p\theta_1+\alpha_1)\cos(p\theta_2+\alpha_2)\exp(im\phi)\right] \\ & -\frac{\hat{\boldsymbol{z}}\hat{\boldsymbol{z}}\cdot\boldsymbol{\nabla}\left[\cos(p\theta_1+\alpha_1)\cos(p\theta_2+\alpha_2)\exp(im\phi)\right]}{\mu^2} \\ & +\frac{i\hat{\boldsymbol{z}}}{\mu}\times\boldsymbol{\nabla}\left[\cos(p\theta_1+\alpha_1)\cos(p\theta_2+\alpha_2)\exp(im\phi)\right]\Bigg\} .\end{aligned} \tag{A10}$$

In Eq. (A10) gradients are computed via

$$\boldsymbol{\nabla}_a[\cos(p\theta_i+\alpha_i)] = -p\boldsymbol{\nabla}_a\theta_i\sin(p\theta_1+\alpha_i) \tag{A11}$$

where $\boldsymbol{\nabla}\theta_i$ are computed from Eqs. (A3). The components of the displacement are

$$\begin{aligned}\left(1-\frac{1}{\mu^2}\right)\boldsymbol{\xi}_\varpi &= \frac{\partial\Psi}{\partial\varpi}+\frac{im\Psi}{\mu\varpi} \approx \frac{\partial\Psi}{\partial\varpi} \\ \boldsymbol{\xi}_z &= \frac{\partial\Psi}{\partial z} \\ \left(1-\frac{1}{\mu^2}\right)\boldsymbol{\xi}_\phi &= \frac{im\Psi}{\varpi}+\frac{i}{\mu}\frac{\partial\Psi}{\partial\varpi} \approx \frac{i\xi_\varpi}{\mu} ,\end{aligned} \tag{A12}$$

[2] However, we use the convention that the mode is proportional to $\exp(+i\omega t)$; Arras et al. (2003) employed modes $\propto\exp(-i\omega t)$.

[3] The sign of the last term here is opposite to Eq. (29) in Arras et al. (2003) because of the different sign convention for frequency used here.

where the approximations are valid within the WKB limit. The necessary derivatives are

$$\frac{\partial\Psi}{\partial\varpi} = -\frac{p\sqrt{1-\mu^2}e^{i(m\phi+\omega t)}}{2\sqrt{\rho\sin\theta_1\sin\theta_2}}\left(\frac{\sin\eta_+}{\sin\tilde\theta_+} - \frac{\sin\eta_-}{\sin\tilde\theta_-}\right)$$
$$\frac{\partial\Psi}{\partial z} = \frac{p|\mu|e^{i(m\phi+\omega t)}}{2\sqrt{\rho\sin\theta_1\sin\theta_2}}\left(\frac{\sin\eta_+}{\sin\tilde\theta_+} + \frac{\sin\eta_-}{\sin\tilde\theta_-}\right) \tag{A13}$$

where $\eta_\pm = p(\theta_2 \pm \theta_1) + \alpha_2 \pm \alpha_1$ and $\tilde\theta_\pm = \theta_2 \pm \theta_1$.

Normalization Integral

Define

$$N \equiv \int d^3x\rho|\boldsymbol{\xi}|^2 \ ; \tag{A14}$$

using Eqs. (A12) and (A13) as well as Eq. (A4) we get

$$N = \frac{\pi|\mu|p^2}{(1-\mu^2)^2}\int d\theta_1 d\theta_2 \left(\frac{\sin^2\eta_+\sin\tilde\theta_-}{\sin\tilde\theta_+} + \frac{\sin^2\eta_-\sin\tilde\theta_+}{\sin\tilde\theta_-} - 2\mu^2\sin\eta_+\sin\eta_-\right) \ . \tag{A15}$$

We replace the rapidly oscillating terms $\sin^2\eta_\pm \to \frac{1}{2}$ and $\sin\eta_+\sin\eta_- \to 0$. Judiciously substitute $\sin\tilde\theta_\pm = \sin(\tilde\theta_\mp \pm 2\theta_1) = \sin\tilde\theta_\mp\cos 2\theta_1 \pm \cos\tilde\theta_\mp \sin 2\theta_1$, with which the integral becomes

$$N = \frac{\pi p^2|\mu|}{2(1-\mu^2)^2}\int_0^{\theta_{|\mu|}} d\theta_1 \int_{\theta_{|\mu|}}^{\pi-\theta_{|\mu|}} d\theta_2 \left[2\cos 2\theta_1 + \sin 2\theta_1\left(\frac{\cos\tilde\theta_-}{\sin\tilde\theta_-} - \frac{\cos\tilde\theta_+}{\sin\tilde\theta_+}\right)\right] \ . \tag{A16}$$

The remaining integrals may all be done analytically; the result is

$$N = \frac{\pi^2p^2\mu^2}{(1-\mu^2)^{3/2}} \ . \tag{A17}$$

See Arras et al. (2003), Eq. (47); the exact result for Bryan modes is in Brink et al. (2004), §II.D.

Damping in a Viscous Bondary Layer

For evaluating damping via boundary layer viscosity, we will need to compute the surface integral of $\rho|\boldsymbol{\xi}|^2$. We use Eq. (A2) to write $\tilde\theta_\pm = \theta_2 \pm \theta_1 = \cos^{-1}(r\cos\theta_\pm)$ and therefore

$$\rho|\boldsymbol{\xi}|^2 \approx \frac{p^2\mu^2}{2(1-\mu^2)\sin\theta_1\sin\theta_2}\left\{\frac{\sin^2[p\cos^{-1}(r\cos\theta_+) - p\pi]}{1-r^2+r^2\sin^2\theta_+} + \frac{\sin^2[p\cos^{-1}(r\cos\theta_-)]}{1-r^2+r^2\sin^2\theta_-}\right\}$$
$$-\frac{\sigma\mu^4\sin[p\cos^{-1}(r\cos\theta_+) - p\pi]\sin[p\cos^{-1}(r\cos\theta_-)]}{(1-\mu^2)\sin\theta_1\sin\theta_2\sin[\cos^{-1}(r\cos\theta_+)]\sin[\cos^{-1}(\cos\theta_-)]} \ . \tag{A18}$$

where $\sigma = +1$ for even parity and $\sigma = -1$ for odd parity, and in the first two terms we used $\sin^2[\cos^{-1}(r\cos\theta_\pm)] = 1 - r^2\cos^2\theta_\pm = 1 - r^2 + r^2\sin^2\theta_\pm$. Using Eq. (A1) to eliminate $\sin\theta_1\sin\theta_2$ we get

$$\frac{r^2}{2N}\int d\Omega\rho|\boldsymbol{\xi}^2| \approx \frac{r}{2\pi}\int_0^\pi d\theta\left\{\frac{\sin^2\{p[\cos^{-1}(r\cos\theta_+) - \pi\}}{1-r^2+r^2\sin^2\theta_+} + \frac{\sin^2[p\cos^{-1}(r\cos\theta_-)]}{1-r^2+r^2\sin^2\theta_-}\right\}$$
$$-\frac{\sigma r}{\pi}\int_0^\pi \frac{d\theta\sin\{p[\cos^-(r\cos\theta_+) - \pi\}\sin[p\cos^{-1}(r\cos\theta_-)]}{\sqrt{(1-r^2+r^2\sin^2\theta_+)(1-r^2+r^2\sin^2\theta_-)}} \tag{A19}$$

where $\sigma = +1$ for even parity and $\sigma = -1$ for odd parity. In the notation of Eq. (7), $R(dE_D/dr)_b/E_D$ is *twice* Eq. (A19). In Eq. (A19), the integrands in $\{\cdots\}$ have large values near $\theta_+ = \pi$ and $\theta_- = 0$, respectively. Writing $\theta_+ = \pi + \delta$ and $\theta_- = \delta$, we get $1 - r^2 + r^2\sin^2\theta_\pm \approx 1 - r^2 + r^2\delta^2$, and $\cos^{-1}(r\cos\theta_+) = \pi - \sqrt{1-r^2+r^2\delta^2}$ and $\cos^{-1}(r\cos\theta_-) = \sqrt{1-r^2+r^2\delta^2}$, respectively, near those points; in both cases, then

$$\frac{\sin^2[p\cos^{-1}(r\cos\theta)]}{1-r^2+r^2\sin^2\theta} \approx \frac{\sin^2[p\sqrt{1-r^2+r^2\delta^2}]}{1-r^2+r^2\delta^2} = \frac{\sin^2[p\sqrt{1-r^2}(1+u^2)^{1/2}]}{(1-r^2)(1+u^2)} \ , \tag{A20}$$

where $u^2 = r^2\delta^2/(1-r^2)$. If $1 - r^2 \ll 1$ we can approximate the integrals by

$$\frac{1}{r\sqrt{1-r^2}}\int_{-\infty}^{+\infty}\frac{du\sin^2[p\sqrt{1-r^2}(1+u^2)^{1/2}]}{1+u^2} \equiv \frac{\pi K(p\sqrt{1-r^2})}{r\sqrt{1-r^2}} \ ; \tag{A21}$$

$$K(z) \approx \begin{cases} z & \text{if } z \ll 1 \\ \frac{1}{2} & \text{if } z \gg 1 \end{cases} \tag{A22}$$

Since the contribution to the integral from the cross term is smaller, we find that

$$\frac{r^2}{2N}\int d\Omega\rho|\boldsymbol{\xi}^2| \approx \frac{K(p\sqrt{1-r^2})}{\sqrt{1-r^2}} \tag{A23}$$

for $1 - r^2 \ll 1$. The damping rate from a viscous shearing boundary layer is therefore proportional to $R(dE_D/dr)_b/2E_D \simeq K(p\sqrt{1-r^2})/\sqrt{1-r^2}$; at large p, the damping rate is proportional to $1/2\sqrt{1-r^2}$, which is independent of p.

Shear Viscosity Damping within $r = r_b$

For computing shear viscosity damping, we need the square of the shear tensor:

$$\sigma_{ab} = \frac{\partial\xi_a}{\partial x_b} + \frac{\partial\xi_b}{\partial x_b} - \frac{2\delta_{ab}\boldsymbol{\nabla}\cdot\boldsymbol{\xi}}{3} \approx \frac{\partial\xi_a}{\partial x_b} + \frac{\partial\xi_b}{\partial x_b} \equiv S_{ab} + S_{ba} \tag{A24}$$

where the approximation $\boldsymbol{\nabla}\cdot\boldsymbol{\xi} = 0$ holds in WKB. Using Eq. (A12) we can compute the shear tensor components; then

$$\sigma^2 \equiv \sum_{ab}\sigma_{ab}\sigma_{ab} = \left[\frac{8\mu^4+2\mu^2}{(1-\mu^2)^2}\right]\left(\frac{\partial^2\Psi}{\partial\varpi^2}\right)^2 + \frac{2(1-3\mu^2+4\mu^4)}{(1-\mu^2)^2}\left(\frac{\partial^2\Psi}{\partial\varpi\partial z}\right)^2 . \tag{A25}$$

In the WKB limit

$$\frac{\partial^2\Psi}{\partial u\partial v} = -\frac{p^2}{\sqrt{\rho\sin\theta_1\sin\theta_2}}\Bigg[\cos(p\theta_1+\alpha_1)\cos(p\theta_2+\alpha_2)\left(\frac{\partial\theta_1}{\partial u}\frac{\partial\theta_1}{\partial v}+\frac{\partial\theta_2}{\partial u}\frac{\partial\theta_2}{\partial v}\right)$$
$$-\sin(p\theta_1+\alpha_1)\sin(p\theta_2+\alpha_2)\left(\frac{\partial\theta_1}{\partial u}\frac{\partial\theta_2}{\partial v}+\frac{\partial\theta_1}{\partial v}\frac{\partial\theta_2}{\partial u}\right)\Bigg] ; \tag{A26}$$

using Eqs. (A3) and $\sin^2(\theta_1 \pm \theta_2) = 1 - r^2\cos^2\theta_\pm$ we get

$$\sigma^2 = \frac{p^4\mu^2}{2\rho r\sin\theta(1-\mu^2)^{3/2}}\Bigg\{\frac{\cos^2[p(\theta_1+\theta_2)+\alpha_1+\alpha_2]}{(1-r^2\cos^2\theta_+)^2} + \frac{\cos^2[p(\theta_1-\theta_2)+\alpha_1-\alpha_2]}{(1-r^2\cos^2\theta_-)^2}$$
$$+\frac{(4\mu^2(3-4\mu^2)\cos^2[p(\theta_1+\theta_2)+\alpha_1+\alpha_2]\cos^2[p(\theta_1-\theta_2)+\alpha_1-\alpha_2]}{(1-r^2\cos^2\theta_+)(1-r^2\cos^2\theta_-)}\Bigg\} ; \tag{A27}$$

the terms on the second line of Eq. (A27) oscillate rapidly and will be dropped in our detailed calculation of the damping rate.

We will assume that the main contribution to the damping rate is from the core of the neutron star, $r \le r_b < 1$; this means that we will never encounter the *exactly two* points on the surface where Eq. (A27) is singular. Fig. 6 in Shternin & Yakovlev (2008) suggests that the shear viscosity grows perhaps linearly in the core of a neutron star, so we let $\eta = \eta_{core}\rho$ in the core, where η_{core} is independent of density; this roughly cancels the $1/\rho$ factor in Eq. (A27) from the WKB form of the modes. For large values of p, we approximate the first two terms in Eq. (A27) by replacing $\cos^2[p(\theta_1 \pm \theta_2) + \alpha_1 \pm \alpha_2] \to \frac{1}{2}$, and drop the cross term entirely. Then

$$\int d^3r\rho\sigma^2 \approx \frac{\pi p^4\mu^2}{2(1-\mu^2)^{3/2}}\int_0^\pi d\theta\int_0^{r_b} dr\, r\left[\frac{1}{(1-r^2\cos^2\theta_+)^2}+\frac{1}{(1-r^2\cos^2\theta_-)^2}\right]$$
$$= \frac{\pi p^4 r_b^2\mu^2}{4(1-\mu^2)^{3/2}}\sum_{s=\pm}\int_0^{2\pi}\frac{d\theta}{1-r_b\cos\theta_s} \tag{A28}$$

The integrals involved are all $2\pi/\sqrt{1-r_b^2}$, so the final result is

$$\int d^3r\rho\sigma^2 = \frac{\pi^2 p^4 r_b^2\mu^2}{(1-\mu^2)^{3/2}\sqrt{1-r_b^2}} \tag{A29}$$

Dividing by N and multiplying by η_{core} gives the damping rate

$$\gamma_{core} = \frac{\eta_{core}p^2(r_b/R)^2}{R^2\sqrt{1-(r_b/R)^2}} \tag{A30}$$

where we have restored dimensional units. Note that Eq. (A30) would diverge as $r_b \to R$. That case requires a more careful treatement.

Brink et al. (2004) included the entire star in the calculation of shear damping: Eq. (31) in that paper is an accurate analytic fit, which we reproduce here: for kinematic viscosity η,

$$\frac{\gamma R^2}{\eta} = \frac{2n+1}{3}\left[(n+3)(n-2) - \frac{m(m-2\mu)}{1-\mu^2}\right] \tag{A31}$$

which is approximately $\gamma/\eta = 2n^3/3$ for $n \gg |m|$, which is typical of couplings of large n modes to the R mode. We have also done a WKB calculation that gives $\gamma R^2/\eta \approx 2p^3/3$. That calculation is rather complicated because the result is dominated by contributions from near the special points on the surface where $\cos\theta_1 = \pm\cos\theta_2 = |\mu|$. The procedure is to return to the displacement field $\boldsymbol{\xi}$, introduce approximations valid near the special points, and then compute the shear tensor by direct differentiation. This last step deviates from the strict WKB approximation in that if $\boldsymbol{k}_i = \boldsymbol{\nabla}\theta_i$ it includes terms arising from $\boldsymbol{\nabla}\boldsymbol{k}_i$ that would be discarded ordinarily. The expression that results can then be integrated analytically, and the result is what we quoted above.

To get the expression for shear viscosity damping in the main text, we divide the star into a core out to r_b and crust outside r_b, with separate viscosities η_{core} and η_{crust}, respectively.

TOY MODEL FOR DISPLACEMENT EVOLUTION AS SHEAR MODULUS RISES

We consider the transition region of thickness Δr within which the shear modulus $\mu(x)$ rises from zero to its value in the crystalline crust. We ignore density variation, and consider planar displacement fields only with $\boldsymbol{\nabla}\cdot\boldsymbol{\xi} = 0$. We orient the radial direction along x and define $c_t^2(x) = \mu(x)/\rho$.

We assume that displacements are proportional to functions of x times $\exp[i(k_y y + k_z z) - i\omega t]$; the divergenceless condition implies that ξ_y and ξ_z are both $\mathcal{O}(|\partial\xi_x/\partial x|)$ and hence much larger than ξ_x. Then if we systematically ignore $k_{y,z}$ compared with $\partial/\partial x$ in this region both ξ_y and ξ_z obey the approximate linear differential equation

$$-\omega^2\xi = \frac{\partial}{\partial x}\left(c_t^2\frac{\partial\xi}{\partial x}\right) \ . \tag{B1}$$

This equation describes the evolution of the jumps in these displacement components. Let $c_t^2 = c_{t,S}^2 f(u)$, where within the layer $x = x_{inner} + u\Delta r$ and in the solid $c_t^2 = c_{t,S}^2$. The function $f(u)$ may be determined from microphysics. Written in terms of u Eq. (B1) is

$$0 = \frac{\partial}{\partial u}\left[f(u)\frac{\partial\xi}{\partial u}\right] + \frac{\omega^2(\Delta r)^2\xi}{c_{t,S}^2} \equiv \frac{\partial}{\partial u}\left[f(u)\frac{\partial\xi}{\partial u}\right] + q^2\xi \ . \tag{B2}$$

Provided that both $f(u)$ and $\xi(u)$ are monotonic, we can regard ξ as a function of f.

Realistically, we would solve Eq. (B2) for a specified $f(u)$. To get a rough idea of what a solution might look like, we pursue an illustrative toy calculation: left $\xi = f^p$, where p is some powerlaw index, to get

$$0 = \frac{d^2 f^{1+p}}{du^2} + q^2(1+p)f^p \ ; \tag{B3}$$

rescale so that $g = Af^{1+p}$ to get

$$0 = \frac{d^2 g}{du^2} + g^{\frac{p}{1+p}} \tag{B4}$$

where we have chosen the scaling constant so that $q^2(1+p)A^{\frac{1}{1+p}} = 1$. We solve Eq. (B4) with $g = 0$ at $u = 0$ but $(dg/du)_0 \neq 0$; we impose the condition that $(dg/du)_1 = 0$ at $u = 1$, which follows since $(df/du)_1 = 0$ for $p > 0$. Consequently $(dg/du)_0$ is an eigenvalue. Since we require that $f(1) = 1$, it follows that $g(1) = A$, so we have $q^2(1+p)[g(1)]^{\frac{1}{1+p}} = 1$, which determines q^2. Thus, it should be clear that this choice of $\xi(f)$ is hardly general, and would only hold for a very specific $f(u)$ and q^2.

Note that Eq. (B4) can be integrated once to yield

$$\frac{dg}{du} = \left(\frac{dg}{du}\right)_0\sqrt{1 - \left(\frac{g}{g_0}\right)^{\frac{1+2p}{1+p}}} \tag{B5}$$

where $g_0^{\frac{1+2p}{1+p}} \equiv (1+2p)(dg/du)_0^2/2(1+p)$. Eq. (B5) can be solved via quadruture. An acceptable solution has $g(1) = g_0$.

The viscous dissipation rate within the layer is

$$\dot{E} = 4\pi\rho_b r_b^2\omega^2\int dx\,\xi\frac{\partial}{\partial x}\left(\eta\frac{\partial\xi}{\partial x}\right) = \frac{4\pi\rho_b r_b^2\omega^2}{\Delta r}\left[\xi\eta(u)\frac{\partial\xi}{\partial u}\bigg|_0^1 - \int_0^1 du\eta(u)\left(\frac{\partial\xi}{\partial u}\right)^2\right] \ . \tag{B6}$$

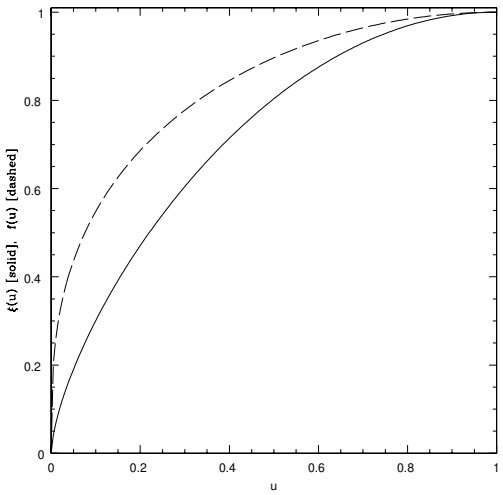

FIG. 2.—: $\xi(u)$ [solid] and $f(u)$ [dashed] for the toy model with $p = 2$. The solution shows that the displacement field changes smoothly within the transition zone from crust to core, with a characteristic length scale $\sim \Delta r$, the thickness of the zone.

Let the kinemaic viscosity be $\eta(u) = \eta_{core}\hat{\eta}(u)$, where $\hat{\eta}(0) = 1$ and $\hat{\eta}(1) = \eta_{crust}/\eta_{core} \ll 1$; we assume $\hat{\eta}(u) \leq 1$ to get an upper bound on $\dot{E}$ Since $\omega\xi = \Delta v[g/g(1)]^{\frac{p}{1+p}}$ in our toy model

$$\dot{E} = -\frac{4\pi p^2 \eta_{core}\rho_b r_b^2(\Delta v)^2}{\Delta r(1+p)^2[g(1)]^{\frac{2p}{1+p}}}\left\{\left[\frac{(1+p)g^{\frac{p-1}{1+p}}}{p}\frac{dg}{du}\right]_0 + \int_0^1 \frac{du\hat{\eta}(u)}{[g(u)]^{\frac{2}{1+p}}}\left(\frac{dg(u)}{du}\right)^2\right\} . \tag{B7}$$

Since $g(u) \sim u$ at $u \ll 1$ the integral diverges for $p \leq 1$

We have solved Eq. (B4) for $p = 2$; the eigenvalue is $(dg/du)_0 \approx 0.135164405635$, and $g(1) \approx 0.0811944$; consequently, $3\omega^2(\Delta r)^2[g(1)]^{1/3}/c_{t,S}^2 = 1$, or $c_{t,S} = 1.14\omega\Delta r = 3.5 \times 10^7\,\mathrm{cm\,s^{-1}}\,\nu_{500}(\omega/\Omega)(\Delta r/100\,\mathrm{m})$, which is a plausible value but cannot be right for all modes, each of which has its own value of ω. For a given $f(u)$ the function $\xi(f)$ must differ among modes and generally the problem does not scale as it does when $\xi(f) = f^p$. Nevertheless, this toy model illustrates the salient features of how a transition might occur. The solution is shown in Fig. 2. The dissipation rate in this model is $\dot{E} \leq 4\pi\eta_{core}\rho_b r_b^2(\Delta v)^2/\Delta r \times 1.99$.

We thank J. Brink, J. Cordes, D. Charkrabarty and P. Shternin for helpful correspondence. IW is grateful for past discussions with P. Arras and S. Teukolsky on some of the approximations required to derive the WKB results in Appendix A. RB is grateful to L. S. Finn, B. Owen and P. Jetzer for useful discussions and support. This research was supported in part by NASA ATP grant NNX13AH42G to Cornell University and by NSF grant PHY11-25915 to the Kavli Institute for Theoretical Physics at University of California, Santa Barbara. RB aknowledges current support from the Dr. Tomalla Foundation and the Swiss National Science Foundation. She was previously supported by NSF PHY 09-69857 awarded to the Pennsylvania State University.

REFERENCES

Alpar, M. A., Cheng, A. F., Ruderman, M. A., & Shaham, J. 1982, Nature, 300, 728
Andersson, N. 1998, ApJ, 502, 708, arXiv:gr-qc/9706075
Andersson, N., Comer, G. L., & Glampedakis, K. 2005, Nuclear Physics A, 763, 212, arXiv:astro-ph/0411748
Andersson, N., Kokkotas, K., & Schutz, B. F. 1999, ApJ, 510, 846, arXiv:astro-ph/9805225
Arras, P., Flanagan, E. E., Morsink, S. M., Schenk, A. K., Teukolsky, S. A., & Wasserman, I. 2003, ApJ, 591, 1129, arXiv:astro-ph/0202345
Arzoumanian, Z., Cordes, J. M., & Wasserman, I. 1999, ApJ, 520, 696, arXiv:astro-ph/9811323
Bildsten, L. 1998, ApJ, 501, L89+, arXiv:astro-ph/9804325
Bildsten, L. et al. 1997, ApJS, 113, 367, arXiv:astro-ph/9707125
Bildsten, L., & Ushomirsky, G. 2000, ApJ, 529, L33, arXiv:astro-ph/9911155
Bondarescu, R., Teukolsky, S. A., & Wasserman, I. 2007, Phys. Rev. D, 76, 064019, 0704.0799
——. 2009, Phys. Rev. D, 79, 104003, 0809.3448
Boutloukos, S., & Nollert, H.-P. 2007, Phys. Rev. D, 75, 043007, arXiv:gr-qc/0605044
Brink, J. 2005, PhD thesis, Cornell University, United States – New York
Brink, J., Teukolsky, S. A., & Wasserman, I. 2004, Phys. Rev. D, 70, 124017, arXiv:gr-qc/0409048
——. 2005, Phys. Rev. D, 71, 064029, arXiv:gr-qc/0410072
Brown, E. F. 2000, ApJ, 531, 988, arXiv:astro-ph/9910215
Chakrabarty, D. 2005, in American Institute of Physics Conference Series, Vol. 797, Interacting Binaries: Accretion, Evolution, and Outcomes, ed. L. Burderi, L. A. Antonelli, F. D'Antona, T. di Salvo, G. L. Israel, L. Piersanti, A. Tornambè, & O. Straniero, 71–80
Chakrabarty, D. 2008, in American Institute of Physics Conference Series, Vol. 1068, American Institute of Physics Conference Series, ed. R. Wijnands, D. Altamirano, P. Soleri, N. Degenaar, N. Rea, P. Casella, A. Patruno, & M. Linares, 67–74

Chakrabarty, D. 2012, in COSPAR Meeting, Vol. 39, 39th COSPAR Scientific Assembly, 295
Chandrasekhar, S. 1970, Physical Review Letters, 24, 611
Cook, G. B., Shapiro, S. L., & Teukolsky, S. A. 1994, ApJ, 423, L117+
Cutler, C., Lindblom, L., & Splinter, R. J. 1990, ApJ, 363, 603
Flowers, E., Ruderman, M., & Sutherland, P. 1976, ApJ, 205, 541
Friedman, J. L., & Morsink, S. M. 1998, ApJ, 502, 714, arXiv:gr-qc/9706073
Friedman, J. L., & Schutz, B. F. 1978, ApJ, 222, 281
Glampedakis, K., & Andersson, N. 2006, MNRAS, 371, 1311, arXiv:astro-ph/0607105
Gusakov, M. E., Kaminker, A. D., Yakovlev, D. G., & Gnedin, O. Y. 2004, A&A, 423, 1063, arXiv:astro-ph/0404002
Haskell, B., Andersson, N., & Passamonti, A. 2009, MNRAS, 397, 1464, 0902.1149
Haskell, B., Glampedakis, K., & Andersson, N. 2013, 1307.0985.
Hessels, J. W. T., Ransom, S. M., Stairs, I. H., Freire, P. C. C., Kaspi, V. M., & Camilo, F. 2006, Science, 311, 1901, arXiv:astro-ph/0601337
Heyl, J. 2002, ApJ, 574, L57. arXiv:astro-ph/0206174
Ivanov, P. B., & Papaloizou, J. C. B. 2010, MNRAS, 407, 1609
Kinney, J. B., & Mendell, G. 2003, Phys. Rev. D, 67, 024032, arXiv:gr-qc/0206001
Kojima, Y. 1998, MNRAS, 293, 49, arXiv:gr-qc/9709003
Kojima, Y., & Hosonuma, M. 1999, ApJ, 520, 788, arXiv:astro-ph/9903055
Kolomeitsev, E. E., & Voskresensky, D. N. 2008, Phys. Rev. C, 77, 065808, 0802.1404
Lee, U., & Strohmayer, T. E. 1996, A&A, 311, 155
Levin, Y., & Ushomirsky, G. 2001, MNRAS, 324, 917, arXiv:astro-ph/0006028
Lindblom, L., & Owen, B. J. 2002, Phys. Rev. D, 65, 063006, arXiv:astro-ph/0110558
Lindblom, L., Owen, B. J., & Morsink, S. M. 1998, Physical Review Letters, 80, 4843, arXiv:gr-qc/9803053
Lockitch, K. H., Andersson, N., & Friedman, J. L. 2000, Phys. Rev. D, 63, 024019
Lockitch, K. H., Andersson, N., & Friedman, J. L. 2001, Phys. Rev. D, 63, 024019, arXiv:gr-qc/0008019
Lockitch, K. H., Andersson, N., & Watts, A. L. 2004, Classical and Quantum Gravity, 21, 4661, arXiv:gr-qc/0106088
Lockitch, K. H., & Friedman, J. L. 1999, ApJ, 521, 764, arXiv:gr-qc/9812019
Lockitch, K. H., Friedman, J. L., & Andersson, N. 2003, Phys. Rev. D, 68, 124010
Manchester, R. N., Hobbs, G. B., Teoh, A., & Hobbs, M. 2005, AJ, 129, 1993
Mendell, G. 2001, Phys. Rev. D, 64, 044009, arXiv:gr-qc/0102042
Nayyar, M., & Owen, B. J. 2006, Phys. Rev. D, 73, 084001, arXiv:astro-ph/0512041
Page, D., Lattimer, J. M., Prakash, M., & Steiner, A. W. 2004, ApJS, 155, 623, arXiv:astro-ph/0403657
——. 2009, ArXiv e-prints, 0906.1621
Page, D., Prakash, M., Lattimer, J. M., & Steiner, A. W. 2011, Physical Review Letters, 106, 081101, 1011.6142
Papaloizou, J., & Pringle, J. E. 1978, MNRAS, 182, 423
Passamonti, A., Stavridis, A., & Kokkotas, K. D. 2008, Phys. Rev. D, 77, 024029
Patruno, A., & Watts, A. L. 2012, ArXiv e-prints, 1206.2727
Pons, J. A., Gualtieri, L., Miralles, J. A., & Ferrari, V. 2005, MNRAS, 363, 121, arXiv:astro-ph/0504062
Rezania, V. & Morsink, S. M. 2002, ApJ, 574, 908, arXiv:astro-ph/0111571
Rezzolla, L., Lamb, F., & Shapiro, L. S. 2000, ApJ, 531, L141, arXiv:astro-ph/9911188
Rezzolla, L., Lamb, Markovic, D., F., & Shapiro, L. S. 2000, Phys. Rev. D, 64, 104013, arXiv:astro-ph//010762
Rezzolla, L., Lamb, F., Markovic, D., & Shapiro, L. S. 2000, Phys. Rev. D, 64, 104014, arXiv:astro-ph/010761
Saio, H. 1982, ApJ, 256, 717
Schenk, A. K., Arras, P., Flanagan, É. É., Teukolsky, S. A., & Wasserman, I. 2002, Phys. Rev. D, 65, 024001, arXiv:gr-qc/0101092
Shibazaki, N., Murakami, T., Shaham, J., & Nomoto, K. 1989, Nature, 342, 656
Shternin, P. S., & Yakovlev, D. G. 2008, Phys. Rev. D, 78, 063006, 0808.2018
Shternin, P. S., Yakovlev, D. G., Heinke, C. O., Ho, W. C. G., & Patnaude, D. J. 2011, MNRAS, 412, L108, 1012.0045
Villain, L., Bonazzola, S., & Haensel, P. 2005, Phys. Rev. D, 71, 083001
Wang, J., Zhang, C. M., Zhao, Y. H., Kojima, Y., Yin, H. X., & Song, L. M. 2011, A&A, 526, A88, 1011.5013
Watts, A. L. 2012, ARA&A, 50, 609, 1203.2065
Yakovlev, D. G., Gnedin, O. Y., Kaminker, A. D., & Potekhin, A. Y. 2008, in American Institute of Physics Conference Series, Vol. 983, 40 Years of Pulsars: Millisecond Pulsars, Magnetars and More, ed. C. Bassa, Z. Wang, A. Cumming, & V. M. Kaspi, 379–387
Yakovlev, D. G., Kaminker, A. D., & Levenfish, K. P. 1999, A&A, 343, 650, arXiv:astro-ph/9812366
Yakovlev, D. G., & Pethick, C. J. 2004, ARA&A, 42, 169, arXiv:astro-ph/0402143
Yoshida, S., & Lee, U. 2000a, ApJ, 529, 997, arXiv:astro-ph/9908197
——. 2000b, ApJS, 129, 353, arXiv:astro-ph/0002300
——. 2001, ApJ, 546, 1121, arXiv:astro-ph/0006107
Zhang, C. M., & Kojima, Y. 2006, MNRAS, 366, 137, arXiv:astro-ph/0410248